TECHNICAL RESEARCH REPORT

Kinematics and Workspace of a Novel Three DOF Translational Platform

by L-W. Tsai, G.C. Walsh, and R.E. Stamper

T.R. 96-74

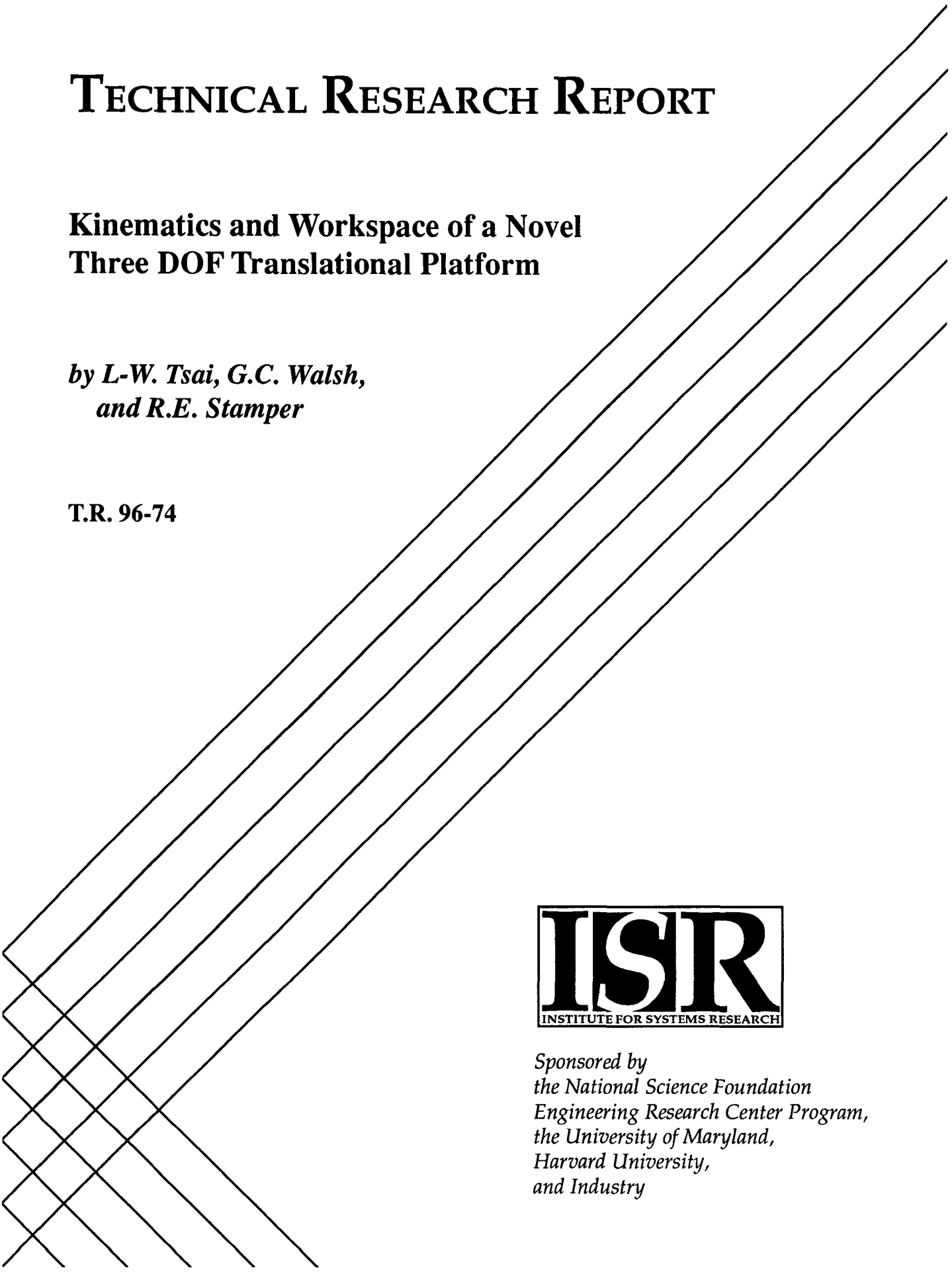

Sponsored by
the National Science Foundation
Engineering Research Center Program,
the University of Maryland,
Harvard University,
and Industry

Kinematics and Workspace of a Novel Three DOF Translational Platform

Lung-Wen Tsai, Gregory C. Walsh, and Richard E. Stamper
Mechanical Engineering Department and
Institute for Systems Research
University of Maryland
College Park, Md 20742

May 29, 1996

Abstract

A novel 3 DOF parallel manipulator is presented that employs only revolute joints and constrains the manipulator output to translational motion. Closed-form solutions are developed for both the inverse and forward kinematics. The inverse kinematics produces four solutions for each leg of the manipulator. In general, the four solutions are realized in only two unique leg configurations. The forward kinematic solution is reduced to a quadratic equation. So that in general, there are two poses the manipulator can assume for a given set of input joint angles. The manipulator workspace is also determined for a manipulator with fixed and moving platforms of the same size.

1 Introduction

The Stewart platform has been studied extensively (Stewart [1], Hunt [2], Griffis and Duffy [3], Innocenti and Parenti-Castelli [4], [5], and Nanua et al. [6]). Other variations of the Stewart platform have also been proposed. Kohli [7] presented six degree-of-freedom (DOF) parallel manipulators that utilize base-mounted rotary-linear actuators; Hudgens and Tesar [8] introduced a six-DOF parallel micromanipulator; Pierrot, et al. [9] developed a high-speed six-DOF parallel manipulator; and recently Tahmasebi and Tsai [10], [11], [12] conceived of a six-DOF parallel minimanipulator with three inextensible limbs. However, most of the

six-DOF parallel manipulators studied to date consist of six limbs which connect a moving platform to a base by spherical joints. These six-limbed manipulators suffer the following disadvantages:

1. Their direct kinematics are difficult to solve.
2. Position and orientation of the moving platform are coupled.
3. Precise spherical joints are difficult to manufacture at low cost.

Note that the only six-limbed, six-DOF parallel manipulators for which closed-form direct kinematic solutions have been reported in the literature are special forms of the Stewart platform (Nanua et al. [6], Grffis and Duffy [3], Innocenti and Parenti-Castelli [5], Lin, et al., [13], Zhang and Song [14]). In these special forms, pairs of spherical joints may present design and manufacturing problems. As to the general Stewart platform, researchers have to resort to numerical techniques for the solutions. Innocenti and Parenti-Castelli [4] developed an exhaustive mono-dimensional search algorithm to find the direct kinematics solutions of the general Stewart platform. Raghavan [15] applied the continuation method and showed that the general Stewart platform has 40 direct kinematics solutions.

A parallel manipulator that addresses two of the listed disadvantages was designed by Clavel and others at the Swiss Federal Institute of Technology [16]. The mainpulator, called the DELTA robot, has four degrees of freedom as designed by Clavel. Three of these degrees of freedom are translational due to the constraints of the kinematic structure of the parallel manipulator. The last degree of freedom is a rotation about an axis perpendicular to the moving platform of the manipulator. The rotational degree of freedom is achieved by an actuator mounted at the base of the manipulator that transmits a rotation to the end effector at the moving platform via a telescopic arm with two universal joints. Closed-form solutions for both the inverse and forward kinematics have been developed for the DELTA robot (Pierrot et al. [18]). Additionally, the position and orientation of the moving platform are uncoupled in the DELTA design. However, the DELTA robot construction does employ spherical joints.

In order to eliminate the spherical joints, a new manipulator was invented by Tsai [17]. It uses only revolute joints to constrain the moving platform to three translational degrees of freedom. In this paper, the kinematics and workspace are developed for a special case of that manipulator, which mimics the motion of the DELTA robot's moving platform. We note that the DELTA robot, after subracting the passive degrees of freedom from each of the spherical-spherical links and the rotation of the end-effector, has exactly three degrees of freedom, while the manipulator designed by Tsai is kinematically an over-constrained mechanism as discussed in the following section.

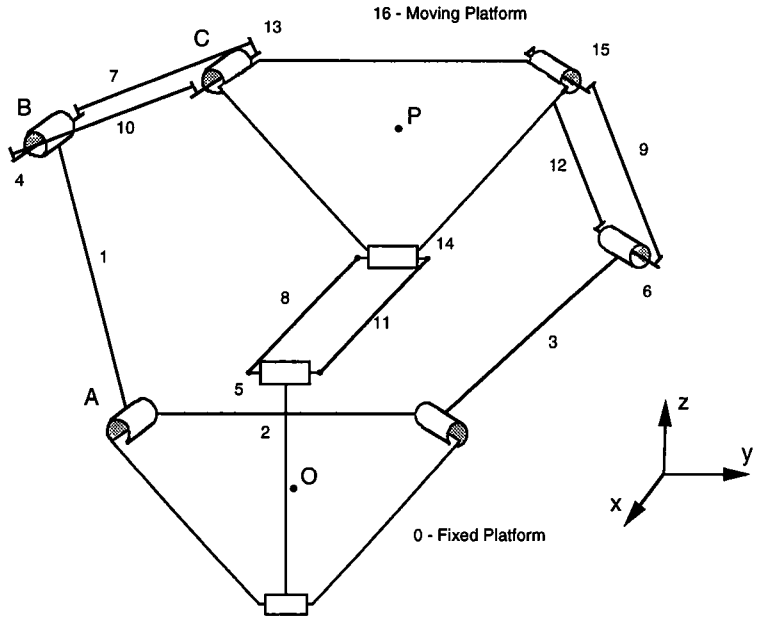

Figure 1: Schematic of the three-DOF manipulator.

2 Description of the Manipulator

A schematic of the special case manipulator being considered is shown in Fig. 1, where the stationary platform is labeled 0 and the moving platform is labeled 16. Three identical limbs connect the moving platform to the stationary platform. Each limb consists of an upper arm and a lower arm. The lower arms are labeled 1, 2, and 3. Each upper arm is a planar four-bar parallelogram: links 4, 7, 10, and 13 for the first limb; 5, 8, 11, and 14 for the second limb; and 6, 9, 12, and 15 for the third limb. For each limb, the upper and lower arms, and the two platforms are connected by three parallel revolute joints. The axes of these revolute joints are perpendicular to the axes of the four-bar parallelogram for each limb. The manipulator shown in Fig. 1 is a special configuration of a more general manipulator invented by Tsai [17]. The more general manipulator includes small offsets in links 4, 5, 6, 13, 14, and 15, as shown in Fig. 2 for links 5 and 14.

The i^{th} leg of the special case manipulator presented in this paper is shown in Fig. 3. A reference frame (XYZ) is attached to the fixed base at point O, located at the center of the fixed platform. The vector $\bar{p}$ is the position vector of point P in the (XYZ) coordinate frame, where P is attached at the center of the moving platform. Another coordinate system (UVW) is attached to the fixed base at A, such that $\bar{u}$ is perpendicular to the axis of rotation of

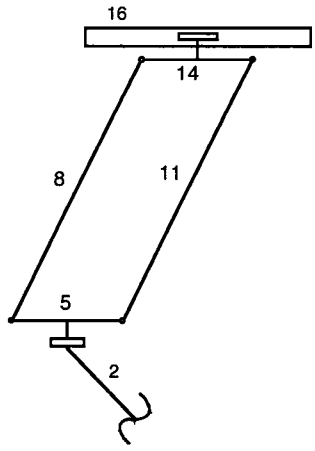

Figure 2: Upper arm configuration for a more general manipulator that facilitates the use of revolute joints.

the joint at A and in the same line as $\overline{OA}$. The angle θ_{0i} is a parameter of the manipulator design and remains constant. The angle θ_{1i} is measured from $\bar{u}$ to $\overline{AB}$. The angle θ_{2i} is defined from $\bar{q}$, a vector pointing from $\overline{AB}$, to $\bar{s}$, which is a vector defined by the intersection of the parallelogram's plane of motion and the U-W plane. The angle θ_{3i} is defined by the angle from $\bar{s}$ to $\overline{BC}$. The angle θ_{4i} is measured from $\bar{t}$, a vector pointing from $\overline{BC}$, to $\overline{CP}$. This angle is fully constrained by the interaction of the three legs so that: $\theta_{4i} = \pi - \theta_{1i} - \theta_{2i}$. Hence, there are nine joint angles, θ_{1i}, θ_{2i}, and θ_{3i} for $i = 1, 2$, and 3, associated with a manipulator posture. For this paper, θ_{11}, θ_{12}, and θ_{13} are considered the actuated joints. Other combinations of actuated joints are also possible, but actuating θ_{11}, θ_{12}, and θ_{13} offers the advantage of attaching each of the actuators to ground.

Considering the manipulator mobility, let F be the degrees of freedom, n the number of links, j the number of joints, f_i the degrees of freedom associated with the i^{th} joint, and $\lambda = 6$, the motion parameter. Then, the degrees of freedom of a mechanism is generally governed by the following mobility equation:

$$F = \lambda(n - j - 1) + \sum_i f_i \tag{1}$$

For the manipulator shown in Fig. 1, $n = 17, j = 21$, and $f_i = 1$ for $i = 1, 2, ..., 21$. Applying Eq. (1) to the manipulator produces: $F = 6(17-21-1)+21 = -9$. Hence, the manipulator is an overconstrained mechanism. However, due to the arrangement of the links and joints,

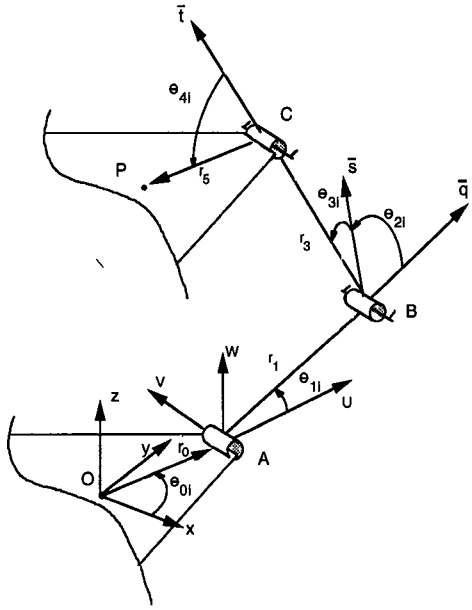

Figure 3: Depiction of the joint angles and link lengths for leg i.

many of the constraints imposed by the joints are redundant and the resulting mechanism does have three translational degrees of freedom. The redundant constraints are a product of the three revolute joints at A, B, and C (as shown in Fig. 1) having parallel axes. As a result, any single limb constrains rotation about the z axis, while the combination of any two limbs constrains rotation about the x and y axes. This leaves the mechanism with three translational degrees of freedom and forces the moving platform to remain in the same orientation as the base. This unique characteristic is useful in many applications such as an X-Y-Z positioning device.

3 Inverse Kinematics

The objective of the inverse kinematics is to develop a set-valued function $f^{-1} : \bar{p} \rightarrow \bar{\theta}$, where $\bar{\theta}$ is the vector consisting of the nine joint angles. An intuitive feel for the solution is developed by considering the problem geometrically. For the inverse kinematics problem, the position of P is given, and in turn the position of C is known. Now consider, the surface generated by the full range of motion of $\overline{CB}$. It is a sphere centered at C. The full range of motion of $\overline{AB}$ is a circle centered about A in the plane of motion of $\overline{AB}$ as shown in Fig. 4. The solution of the inverse kinematics problem is found at the intersection of this circle and

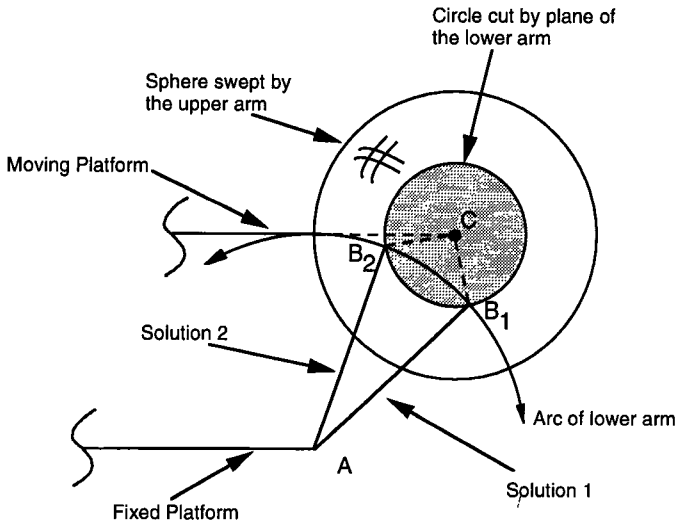

Figure 4: The two inverse kinematic solutions are shown for a single leg from a view looking into the axis of rotation of A.

sphere. Four cases are possible.

1. Generic solution. The circle penetrates the sphere, resulting in two solutions.
2. Singular solution. The circle is tangent to the sphere, resulting in one solution.
3. Singular solution. The circle lies on the sphere, producing an infinite number of solutions. This is unlikely since it requires the moving and stationary platforms to occupy the same plane simultaneously.
4. No real solution. The circle and the sphere may not intersect at all.

With the geometry of the problem in mind, the algebraic solution is developed with the joint angles and link lengths defined in Fig. 3. The position vector of point P for leg i is given by $\bar{p}_i = [p_{xi}, p_{yi}, p_{zi}]^T$:

$$\bar{p}_i = R_i \bar{q}_i \tag{2}$$

where:

$$R_i = \begin{bmatrix} \cos(\theta_{0i}) & -\sin(\theta_{0i}) & 0 \\ \sin(\theta_{0i}) & \cos(\theta_{0i}) & 0 \\ 0 & 0 & 1 \end{bmatrix},$$

$$\bar{q}_i = \begin{bmatrix} r_0 - r_5 + r_1\cos(\theta_{1i}) + r_3\cos(\theta_{3i})\cos(\theta_{1i}+\theta_{2i}) \\ r_3\sin(\theta_{3i}) \\ r_1\sin(\theta_{1i}) + r_3\cos(\theta_{3i})\sin(\theta_{1i}+\theta_{2i}) \end{bmatrix}$$

for $i = 1, 2, 3$. Equation (2) can be written as:

$$\tilde{c}_i = \begin{bmatrix} r_1\cos(\theta_{1i}) + r_3\cos(\theta_{3i})\cos(\theta_{1i}+\theta_{2i}) \\ r_3\sin(\theta_{3i}) \\ r_1\sin(\theta_{1i}) + r_3\cos(\theta_{3i})\sin(\theta_{1i}+\theta_{2i}) \end{bmatrix} \tag{3}$$

where $\tilde{c}_i = [c_{ui}, c_{vi}, c_{wi}]^T$ defines the position vector of point C in the UVW coordinate frame:

$$\tilde{c}_i = \begin{bmatrix} \cos(\theta_{0i}) & \sin(\theta_{0i}) & 0 \\ -\sin(\theta_{0i}) & \cos(\theta_{0i}) & 0 \\ 0 & 0 & 1 \end{bmatrix} \bar{p}_i + \begin{bmatrix} r_5 - r_0 \\ 0 \\ 0 \end{bmatrix}.$$

Hence, θ_{3i} is immediately found by solving the second element of Eq. (3):

$$\theta_{3i} = \arcsin\left(\frac{c_{vi}}{r_3}\right), \tag{4}$$

resulting in two possible solutions for θ_{3i}. However, later it is shown that either of the two solutions for θ_{3i} results in the same physical pose for leg i.

With θ_{3i} determined, an equation with θ_{1i} as the only unknown is generated by summing the squares of $c_{u,i}$ and $c_{w,i}$, eliminating θ_{2i}:

$$r_3^2\cos^2(\theta_{3i}) = [c_{ui} - r_1\cos(\theta_{1i})]^2 + [c_{wi} - r_1\sin(\theta_{1i})]^2. \tag{5}$$

Substituting θ_{3i} into Eq. (5) produces:

$$r_3^2 = c_{ui}^2 + c_{vi}^2 + c_{wi}^2 + r_1^2 - 2r_1\left[c_{ui}\cos(\theta_{1i}) + c_{wi}\sin(\theta_{1i})\right]. \tag{6}$$

To transform Eq. (6) into a polynomial expression, a half angle tangent substitution is defined:

$$t_{1i} = \tan\left(\frac{\theta_{1i}}{2}\right), \tag{7}$$

producing the following relationships, provided that $\theta_{1i} \neq \pm\pi$:

$$\sin(\theta_{1i}) = \tfrac{2t_{1i}}{1+t_{1i}^2} \quad \text{and} \quad \cos(\theta_{1i}) = \tfrac{1-t_{1i}^2}{1+t_{1i}^2}\ . \tag{8}$$

Substituting the relationships from (8) into (6), produces the following quadratic equation in t_{1i}:

$$a_i t_{1i}^2 + b_i t_{1i} + d_i = 0 \tag{9}$$

where:

$$\begin{aligned} a_i &= c_{ui}^2 + c_{vi}^2 + c_{wi}^2 + r_1^2 - r_3^2 + 2r_1 c_{ui} \\ b_i &= -4r_1 c_{wi} \\ d_i &= c_{ui}^2 + c_{vi}^2 + c_{wi}^2 + r_1^2 - r_3^2 - 2r_1 c_{ui}\ . \end{aligned}$$

Equation (9) is then solved for θ_{1i} in terms of only known parameters:

$$\theta_{1i} = 2\arctan\left(\frac{-b_i \pm \sqrt{b_i^2 - 4a_i d_i}}{2a_i}\right). \tag{10}$$

Two solutions for θ_{1i} are produced by Eq. (9). These two solutions are independent of the value of θ_{3i} which was determined from Eq. (4). This results in four solution sets for θ_{1i} and θ_{3i}.

Once θ_{1i} and θ_{3i} are known, θ_{2i} is determined by back substitution into Eq. (3). For each of the four solution sets of θ_{1i} and θ_{3i} there is a single value obtained for θ_{2i}. Moreover, for each solution of θ_{1i}, the two associated values of θ_{2i} differ by π, while the sum of the two associated values of θ_{3i} is π. By virtue of these relationships and the geometry of the leg, each leg assumes the same physical pose for each unique θ_{1i}. Hence, for each leg, the four solution sets are realized in only two distinct poses.

The inverse kinematics solution is tested for special cases by examining Eq. (9). If $b_i^2 - 4a_i d_i > 0$, then the two solutions correspond to the configuration where the circle swept by $\overline{AB}$ intersects the sphere swept by $\overline{CB}$ in two locations. If $b_i^2 - 4a_i d_i = 0$, then the circle and sphere are tangent, and the manipulator is in a singular position. If $b_i^2 - 4a_i d_i < 0$, then the circle and sphere do not intersect and there are no real solutions. If $a_i = b_i = d_i = 0$, then the circle lies on the sphere, and there are an infinite number of solutions.

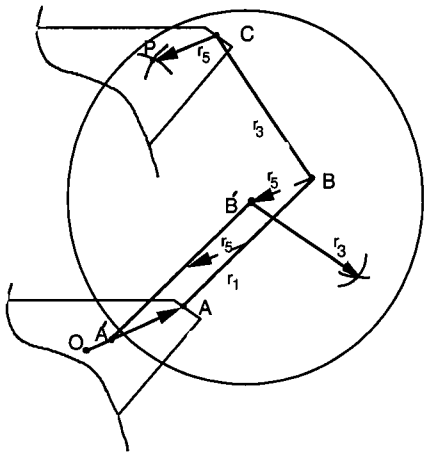

Figure 5: The sphere created by P's range of motion.

4 Forward Kinematics

For the forward kinematics analysis, the input joint angles are θ_{11}, θ_{12}, and θ_{13}. Given these joint angles, a set valued map $f : \theta_{1i} \rightarrow \bar{p}$ is developed for $i = 1, 2$, and 3.

First, consider the surface composed of all possible locations of P for leg i with a known θ_{1i}. The surface is a sphere centered at B', which is a distance r_5 from B in the direction of $\overline{CP}$, as shown in Fig. 5. Now, consider all three legs. P must simultaneously fall on all the spheres created by the sweep of P for each leg. The intersection of these three spheres represents the solution to the forward kinematics problem. In the generic case, there are two solutions, since the intersection of two of the spheres forms a circle, which is generally intersected by the third sphere in two locations as shown in Fig. 6. Four cases are possible.

1. Generic solution. The two solutions are realized at the intersection of a circle and a sphere.

2. Singular solution. One sphere is tangent to the circle of intersection of the other two spheres, hence there is only one solution possible.

3. Singular solution. The centers of any two spheres coincide, resulting in an infinite number of solutions. This is an unlikely configuration for most practical embodiments of the manipulator, except for the situation when $\theta_{11} = \theta_{12} = \theta_{13} = \frac{\pi}{2}$.

4. No solution. The three spheres do not intersect at a common point.

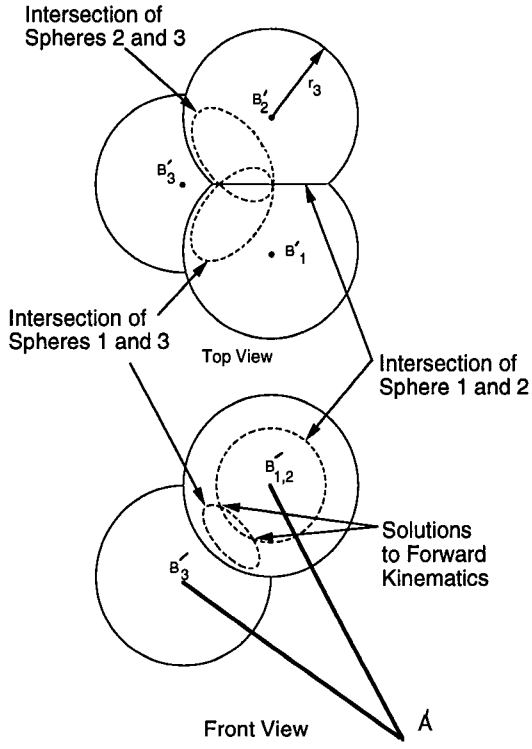

Figure 6: The two forward kinematic solutions are shown at the intersection of the spheres created by the range of motion of P for each leg.

Algebraically, the solution is found by writing the equations that describe the three spheres and then solving those equations for the points of intersection. An equation for the sphere swept by point P for leg i is:

$$\begin{aligned} r_3^2 = {} & p_x^2 + p_y^2 + p_z^2 - 2p_z r_1 \sin(\theta_{1i}) - 2p_x \cos(\theta_{0i}) \left[r_1 \cos(\theta_{1i}) + r_0 - r_5\right] \\ & - 2p_y \sin(\theta_{0i}) \left[r_1 \cos(\theta_{1i}) + r_0 - r_5\right] + \left[r_1 \cos(\theta_{1i}) + r_0 - r_5\right]^2 + r_1^2 \sin^2(\theta_{1i}) \end{aligned} \tag{11}$$

for i=1,2, and 3.

The plane that contains the circle of intersection created by the spheres of leg 1 and leg j, where $j = 2$ and 3, is found by subtracting Eq. (11) for $i = 1$ from Eq. (11) for $i = j$:

$$a_{1j} p_x + b_{1j} p_y + c_{1j} p_z + d_{1j} = 0 \tag{12}$$

where:

$$\begin{aligned} a_{1j} = {} & 2\cos(\theta_{0j}) \left[r_1 \cos(\theta_{1j}) + r_0 - r_5\right] \\ & - 2\cos(\theta_{01}) \left[r_1 \cos(\theta_{11}) + r_0 - r_5\right] \\ b_{1j} = {} & 2\sin(\theta_{0j}) \left[r_1 \cos(\theta_{1j}) + r_0 - r_5\right] \\ & - 2\sin(\theta_{01}) \left[r_1 \cos(\theta_{11}) + r_0 - r_5\right] \\ c_{1j} = {} & 2r_1 \sin(\theta_{1j}) - 2r_1 \sin(\theta_{11}) \\ d_{1j} = {} & \left[r_1 \cos(\theta_{11}) + r_0 - r_5\right]^2 + r_1^2 \sin^2(\theta_{11}) \\ & - \left[r_1 \cos(\theta_{1j}) + r_0 - r_5\right]^2 - r_1^2 \sin^2(\theta_{1j}). \end{aligned}$$

Equation (12) for $j = 2$ and 3 provides a system of equations that is linearly independent as long as the centers of the spheres are not colinear, which is unlikely to be realized in practical embodiments of the manipulator. This system of equations defines a line in $\mathbb{R}^3$ that must contain point P if there is a real solution. The intersection of this line with any of the spheres described by Eq. (11) solves the forward kinematics problem. In this case, solving Eq. (12), where $j = 2$ and 3, for p_y and p_z in terms of p_x and then substituting the resulting expressions into Eq. (11) for $i = 1$, yields:

$$k_0 p_x^2 + k_1 p_x + k_2 = 0. \tag{13}$$

The coefficients for the quadratic are:

$$k_0 = 1 + \frac{l_1^2}{l_2^2} + \frac{l_4^2}{l_5^2},$$

$$
\begin{aligned}
k_1 &= \frac{2l_0l_1}{l_2^2} + \frac{2l_3l_4}{l5^2} - 2l_6\cos(\theta_{01}) \\
&\quad - \frac{2l_6l_1}{l_2}\sin(\theta_{01}) - \frac{2r_1l_4}{l_5}\sin(\theta_{11}), \\
k_2 &= l_6^2 - r_3^2 + \frac{l_0^2}{l_2^2} + \frac{l_3^2}{l_5^2} + r_1^2\sin^2(\theta_{11}) \\
&\quad - \frac{2l_0l_6}{l_2}\sin(\theta_{01}) - \frac{2r_1l_3}{l_5}\sin(\theta_{11}),
\end{aligned}
$$

where:

$$
\begin{aligned}
l_0 &= c_{12}d_{13} - c_{13}d_{12}, \\
l_1 &= a_{13}c_{12} - a_{12}c_{13}, \\
l_2 &= b_{12}c_{13} - b_{13}c_{12}, \\
l_3 &= b_{13}d_{12} - b_{12}d_{13}, \\
l_4 &= a_{12}b_{13} - a_{13}b_{12}, \\
l_5 &= b_{12}c_{13} - b_{13}c_{12}, \\
l_6 &= r_1\cos(\theta_{11}) + r_0 - r_5,
\end{aligned}
$$

and where $a_{12}, a_{13}, b_{12}, b_{13}, c_{12}, c_{13}, d_{12}$, and d_{13} are defined in Eq. (12). The values for p_y and p_z that correspond to p_x are found by back substitution into Eq. (12).

The forward kinematics solution is tested for special cases by examining Eqs. (12) and (13). If the system of equations produced by Eq. (12) for $j = 2$ and 3, is linearly dependent, then the centers of the spheres are colinear, resulting in either an infinite number of solutions if the centers are coincident or no solutions if they are not coincident. If $k_1^2 - 4k_0k_2 > 0$, then two solutions are realized where the circle created by the intersection of two spheres is intersected by the third sphere in two places. If $k_1^2 - 4k_0k_2 = 0$, then the circle created by the intersection of two spheres is tangent to the third sphere. If $k_1^2 - 4k_0k_2 < 0$, then the three spheres do not intersect at a common location, and there are no real solutions.

5 Workspace

The manipulator workspace is found by intersecting the workspaces of the individual legs. A surface that bounds the workspace of leg i is found by setting the discriminant of Eq. (10)

equal to 0:

$$b_i^2 - 4a_i d_i = 0, \tag{14}$$

where:

$$\begin{aligned} a_i &= c_{ui}^2 + c_{vi}^2 + c_{wi}^2 + r_1^2 - r_3^2 + 2r_1 c_{ui} \\ b_i &= -4r_1 c_{wi} \\ d_i &= c_{ui}^2 + c_{vi}^2 + c_{wi}^2 + r_1^2 - r_3^2 - 2r_1 c_{ui} \quad . \end{aligned}$$

Equation (14) describes a torus with a central axis that is parallel to the revolute axis of joint A for leg i. Equation (14) is then expressed in a spherical coordinate system with origin O', as shown in Fig. (7). The coordinate transformation is accomplished by applying the following substitutions: $c_{ui} = \rho_i \sin(\alpha)\cos(\beta)$, $c_{vi} = \rho_i \sin(\alpha)\cos(\beta)$, and $c_{wi} = \rho_i \cos(\alpha)$. Assuming that the moving and fixed platforms are the same size so that $r_0 = r_5$, Eq. (14) is rewritten as:

$$\rho_i^4 + k_{2i}\rho_i^3 + k_{1i}\rho_i^2 + k_{0i}\rho_i = 0, \tag{15}$$

where:

$$\begin{aligned} k_{0i} &= -8r_1^2 r_3 \cos(\alpha) - 8r_1 r_3^2 \cos(\alpha), \\ k_{1i} &= 3r_1^2 + 8r_1 r_3 + 2r_3^2 + r_1^2 \cos(2\alpha) \\ &\quad + 4r_1 r_3 \cos(2\alpha) + 2r_3^2 \cos(2\alpha) \\ &\quad + r_1^2 \cos(2\alpha)\cos(2\beta - 2\theta_{0i}) - r_1^2 \cos\left(2\beta - 2\theta_{0i}\right), \\ k_{2i} &= -4\left(r_1 + r_3\right)\cos(\alpha). \end{aligned}$$

A graphical representation of the surface that bounds the manipulator workspace below the XY plane is plotted by finding the minimum distance from the orgin of the spherical coordinate system to the workspace boundry of any of the three legs ρ_i, or the XY plane ρ_{xy}, i.e.

$$\rho = \min\{\rho_1, \rho_2, \rho_3, \rho_{xy}\}, \tag{16}$$

where:

$$\begin{aligned} \rho_i &= \{\rho : \rho^3 + k_{2i}\rho^2 + k_{1i}\rho + k_{0i} = 0, \quad \rho \in \mathbb{R}\}, \\ \rho_{xy} &= \frac{r_1 + r_3}{\cos(\alpha)}, \end{aligned}$$

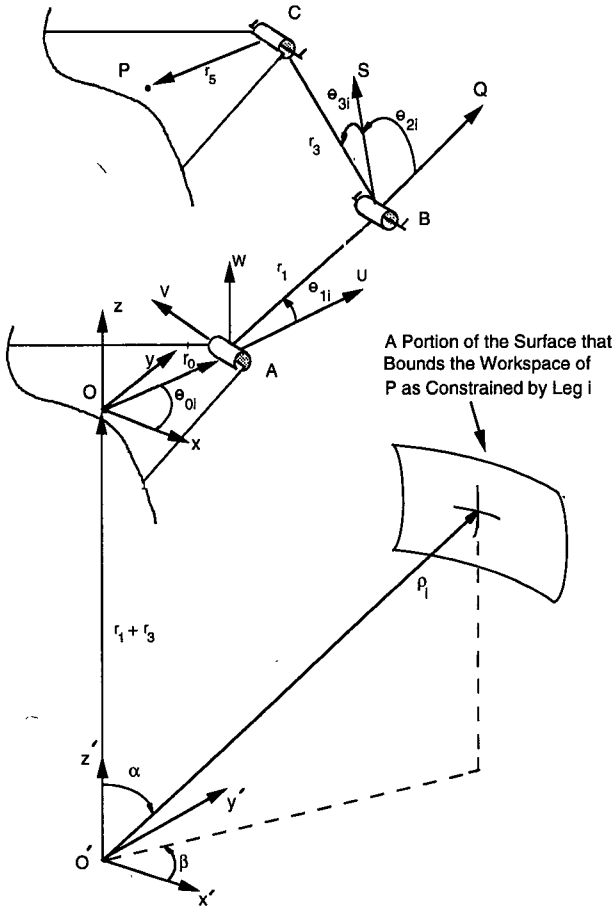

Figure 7: Spherical coordinate system transformation used to determine the workspace of P associated with leg 1.

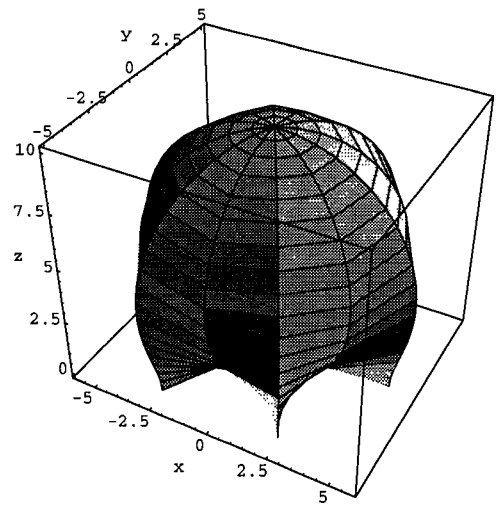

Figure 8: Workspace of manipulator above XY plane with $r_1 = r_3 = 5$.

$$\alpha \in [0, \frac{\pi}{2}],$$
$$\beta \in [0, 2\pi),$$
$$i = 1, 2, 3.$$

The workspace above the XY plane is symetrical to the workspace below the XY plane since the manipulator kinematics are symetrical about the fixed platform. However, every point on the XY plane is a self collision, so the usual workspace consists of points either above or below the XY plane.

The workspace boundry above the XY plane for a manipulator with $r_1 = r_3 = 5$ is shown in Fig. (8). The workspace above the XY plane for a manipulator with $r_1 = 4$ and $r_3 = 6$ is shown in Fig. (9) with a quarter removed to provide a view of the void at the origin that is present whenever $r_1 \neq r_3$.

6 Conclusion

In this paper, a novel parallel manipulator with three translational degrees of freedom is presented. The general design of the manipulator is discussed, along with the mobility that results from the unique link and joint configuration of the manipulator. Closed-formed solutions for both the forward and inverse kinematics are also developed. These solutions demonstrate that in general, there are two possible poses for the forward kinematics, and

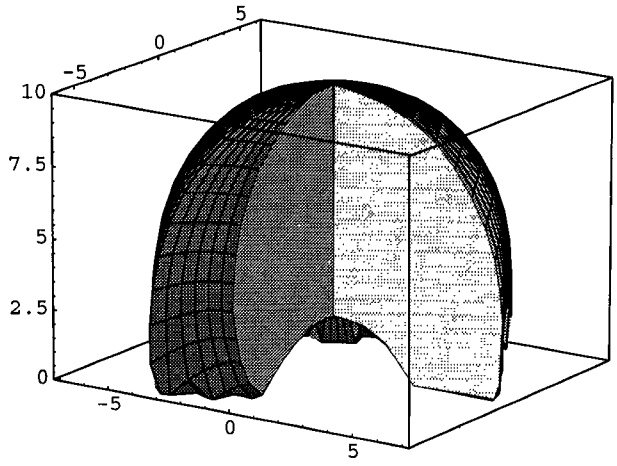

Figure 9: Workspace of manipulator above XY plane with $r_1 = 4$ and $r_3 = 6$.

two possible poses for each leg for the inverse kinematics. A geometric approach for both the forward and inverse kinematics problem is also considered that provides some insights to the nature of inverse and forward kinematics of this manipulator. An approach to determine manipulator workspace is also presented for a manipulator with a fixed and moving platform of the same size.

Acknowledgement

This work was supported in part by the Nation Science Foundation under Grant No. NSF EEC 94-02384. Any opinions, findings, and conclusions or recommendations expressed in this paper are those of the authors and do not no necessarily reflect the views of the supporting agencies.

References

[1] D. Stewart, "A platform with six degrees of freedom," *Proc. Institute of Mechanical Engr.*, vol. 180, pp. 371–386, 1965.

[2] K. H. Hunt, "Structural kinematics of in-parallel-actuated robot-arms," *ASME Journal of Mechanisms, Transmissions, and Automation in Design*, vol. 105, pp. 705–712, 1983.

[3] M. Griffis and J. Duffy, "A forward displacement analysis of a class of Stewart platforms," *Journal of Robotic Systems*, vol. 6, pp. 703–720, 1989.

[4] C. Innocenti and V. Parenti-Castelli, "Forward kinematics of the general 6-6 fully parallel mechanism: An exhaustive numerical approach via a mono-dimensional search algorithm," *ASME Journal of Mechanical Design*, vol. 115, pp. 932–937, 1993.

[5] C. Innocenti and V. Parenti-Castelli, "Direct position analysis of the Stewart platform mechanism," *Mechanism and Machine Theory*, vol. 25, pp. 611–612, 1990.

[6] P. Nanua, K. J. Waldron, and V. Murthy, "Direct kinematic solution of a Stewart platform," *IEEE Transactions on Robotics and Automation*, vol. 6, pp. 438–444, 1990.

[7] D. Kohli, S. H. Lee, K. Y. Tsai, and G. N. Sandor, "Manipulator configurations based on rotary-linear (r-l) actuators and their direct and inverse kinematics," *ASME Journal of Mechanisms, Transmissions, and Automation in Design*, vol. 110, pp. 397–404, 1988.

[8] J. C. Hudgens and D. Tesar, "A fully-parallel six degree-of-freedom micromanipulator: kinematic analysis and dynamic model," *Proceedings of the 20th ASME Biennial Mechanisms Conference*, vol. DE-15.3, pp. 29–37, 1988.

[9] F. Pierrot, A. Fournier, and P. Dauchez, "Toward a fully parallel 6 dof robot for high-speed applications," *International Conference on Robotics and Automation*, pp. 1288–1293, 1991.

[10] F. Tahmasebi and L. W. Tsai, "Six-degree-of-freedom parallel minimanipulator with three inextensible limbs," U.S. Patent, No. 5,279,176, 1994.

[11] F. Tahmasebi and L.W. Tsai, "Closed-form kinematics solution of a new parallel minimanipulator," *ASME Journal of Mechanical Design*, vol. 116, no. 4, pp. 1141–1147, 1994.

[12] F. Tahmasebi and L.W. Tsai, "Workspace and singularity analysis of a novel six-dof parallel mini-manipulator," *Journal of Applied Mechanisms and Robotics*, vol. 1, no. 2, pp. 31–40, 1994.

[13] W. Lin, C.D. Crane, and J. Duffy, "Closed form forward displacement analysis of the 4-5 in parallel platforms," *ASME Journal of Mechanical Design*, vol. 116, pp. 47–53, 1994.

[14] C. Zhang and S.M. Song, "Forward position analysis of nearly general Stewart platforms," *ASME Journal of Mechanism Design*, vol. 116, pp. 54–60, 1994.

[15] M. Raghavan, "The Stewart platform of general geometry has 40 configurations," *ASME Journal of Mechanical Design*, vol. 115, pp. 277–282, 1993.

[16] R. Clavel "Delta, a fast robot with parallel geometry," *Proceedings of the 18th International Symposium on Industrial Robots*, pp. 91–100, 1988.

[17] L. W. Tsai, "Multi-degree-of-freedom mechanisms for machine tools and the like," U.S. Patent Pending, No. 08/415,851, 1995.

[18] F. Pierrot, C. Reynaud, and A. Fournier, "Delta: a simple and efficient parallel robot," *Robotica*, vol. 6, pp. 105–109, 1990.